CERN EP-ADP-OS

A study of the sensitivity to the top quark mass of the top-antitop invariant mass distribution measured at $\sqrt{s} = 8$ TeV with the ATLAS detector

Varsiha Sothilingam

Supervisors: Alexis Vallier, Stefano Camarda

Abstract

In the study of top-antitop events with the ATLAS detector, one can evaluate the sensitivity of the invariant mass distribution of the top quark at a centre of mass energy of $\sqrt{s} = 8$ TeV corresponding to an integrated luminosity of 20.3 fb^{-1} and measured in the lepton + jets decay channel the ATLAS detector. The consideration of higher leading orders of the production of top quarks in these events and investigating statistical behaviour of the data allow us to evaluate the mass of the top quark. Further considerations of bound state effects and electroweak effects allows one to observe how the mass would vary with these considerations.

Geneva, Switzerland

September 5, 2019

1 Introduction

The top quark is the heaviest elementary particle known to date, and the only quark whose mass resides at the electroweak symmetry breaking scale. It is the only fermion whose Yukawa coupling to the Higgs boson is of the order of unity. Among the properties of the top quark, its mass plays a crucial role in the study of the quantum vacuum stability [1], and in the fit of the parameters of the electroweak sector of the Standard Model [2].

The most precise measurements of the top quark exploit the sensitivity of kinematic properties of its decay products, and aim at fully reconstructing the top quark. These methods, which are referred to as direct measurements, rely on general purpose event generators, which include parton showering and hadronisation models. There is a debate whether they yield a measurement of the top quark mass in the pole-mass renormalisation scheme[Paolo Nason], or there is an additional ambiguity in the interpretation of these top quark mass measurements as such[Andre' Hoang].

Alternative measurements, which exploit the sensitivity of cross section, rely on perturbative QCD predictions and allow to determine the mass of the top quark in a well-defined renormalisation scheme. These measurements are less precise, but more unambigously related to the top quark pole mass, and they provide invaluable insight into the issue of relating direct measurements of top quark mass to the pole mass.

The world average of the top quark mass from direct measurements is 172.9 $\pm$ 0.4, whereas for the pole mass from cross-section measurements it is 173.1 $\pm$ 0.9 [5]. These values are averages of the mass values measured by the CDF, D0, CMS, and ATLAS experiments.

The invariant mass distribution of a top-antitop pair produced in hadron collisions is sensitive to the top quark mass, and can be used to measure this parameter in the pole-mass scheme, by using perturbative QCD predictions. Figure 1 shows the differential cross section as a function of the invariant mass of the top-antitop pair, $m_{t\bar{t}}$, for various different values of the top mass, m_t. The cross section is nonzero only above the phase-space threshold of twice m_t, and in the proximity of this threshold the cross section is proportional to the velocity of the top quark.

The data used for this study are $t\bar{t}$ events at a centre-of-mass energy of 8 TeV measured by ATLAS. This study focuses on normalised cross section in order to avoid large theoretical uncertainties on the total cross section due to missing higher orders in perturbative QCD. Moreover the use of normalised cross section avoids correlation of theoretical uncertainty with m_t determination from total cross section measurements and allows combination with the latter.

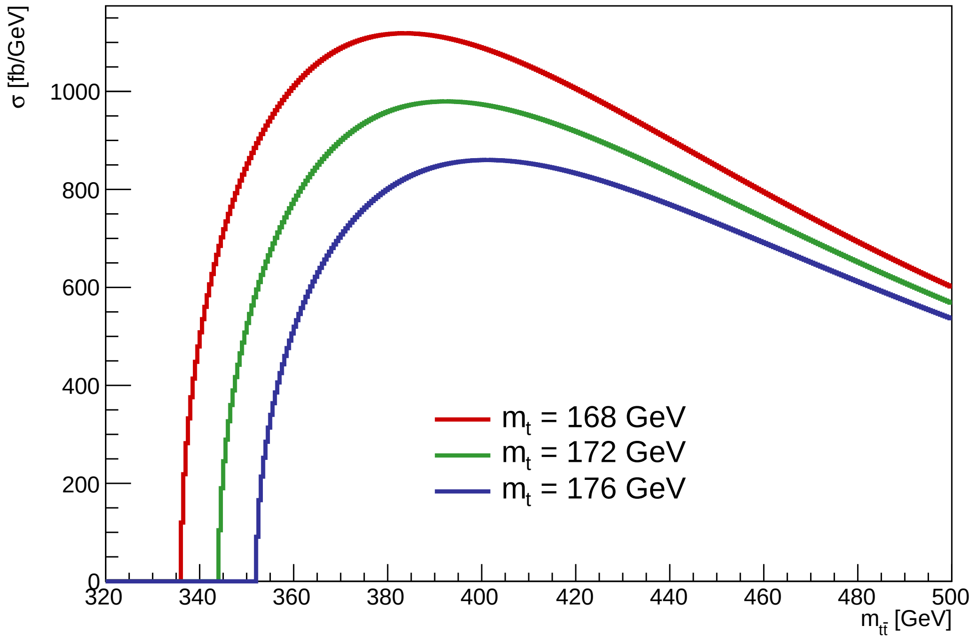

Figure 1: Top pair production cross section as a function of $m_{t\bar{t}}$ in the threshold region for varying mass points in the range 320 GeV to 500 GeV. Predictions are evaluated at leading order.

2 Methodology

The study is based on the ATLAS measurement of differential cross section as a fuction of $m_{t\bar{t}}$ corresponding to an integrated luminosity of 20.3 fb^{-1} and measured in the lepton + jets decay channel [8]. The invariant mass of the $t\bar{t}$ system is poorly reconstructed due to the presence of a neutrino in the final state, The neutrinos transverse momentum is inferred indirectly from momentum balance in the transverse plane and its longitudinal momentum is not measured.

Top-antitop production in hadron collisions at leading order is proportional to α_S^2. Theory predictions are evaluated at next-to-leading-order (NLO), that are $O(\alpha_S^3)$, using `MCFM` [6], whereas next-to-next-to-leading-order (NNLO) predictions ,that are $O(\alpha_S^4)$, are taken from Ref.[8]. The `MCFM` programme, "Monte Carlo for FeMtobarn processes" calculates partonic cross sections for femtobarn level processes at hadron colliders . The NLO MCFM predictions are interfaced to `applGRID` [10] for the fast convolution with parton distribution functions (PDF) and for the fast evaluation of QCD scale variations. The NNLO predictions are interfaced to fastNLO. The fastNLO tables are taken from Ref.[8] which uses a reference mass of m_t= 173.3 GeV. The applGRID tables are created for a range of masses from 168 to 178 GeV.

There are three main steps in applGRID producing grids at NLO. The first step consists in producing vegas preconditioning grid. The vegas algorithm is a type of Monte Carlo integration that is based on importance sampling. It uses probability distribution of the integrand function to concentrate the sampling points into the region with the largest probability [9]. The second step is a phase space sampling which produces a preliminary applGRID used to determine the x and Q^2 ranges of each bin of the $m_{t\bar{t}}$ distribution. The final step releases the PDF convolution on the phase space defined by the previous step. The second and third steps were parallelised to improve the numerical accuracy of the predictions on the HTCondor system available at CERN.

The measured cross section is compared to the theory predictions by means of a χ^2 probability test. The minimum of the χ^2 as a function of m_t yields the measurement of the top quark mass. Its half width at one unit above the minimum provides an estimate of the associated uncertainty.

The χ^2 evaluation and minimisation are performed using the software xFitter- an open-source project for the determination of PDFs.

The χ^2 is defined as $\chi^2 = \sum_{ij}(m_i - \mu_i)^{\mathrm{T}} V^{-1}(m_i - \mu_j)$ where m_i is the measured normalised cross section in bin i, μ_i is the corresponding theory prediction and V is the covariance. In this study we use the mathematically equivalent representation of the χ^2 into nuisance parameters.

Figure 2 shows NLO predictions of the normalised cross section as a function of $m_{t\bar{t}}$ distribution in the bins, corresponding to the ATLAS measurement for varying mass points 168, 172 and 178 GeV, and illustrates the sensitivity to the top quark mass. The up and down variations of the top mass are asymmetric. The asymmetry is likely to be due to the fact that the lowest edge of the first bin is 345 GeV. Hence when m_t is lower than 172.5 GeV the lowest bin edge is higher than the phase-space threshold equal to $2 \cdot m_t$, and part of the cross section ends up in the underflow bin.

3 Physics modelling

Predictions are computed at NLO for different top quark mass in the range 168 to 178 GeV. At each value of the top quark mass, the NLO predictions are corrected

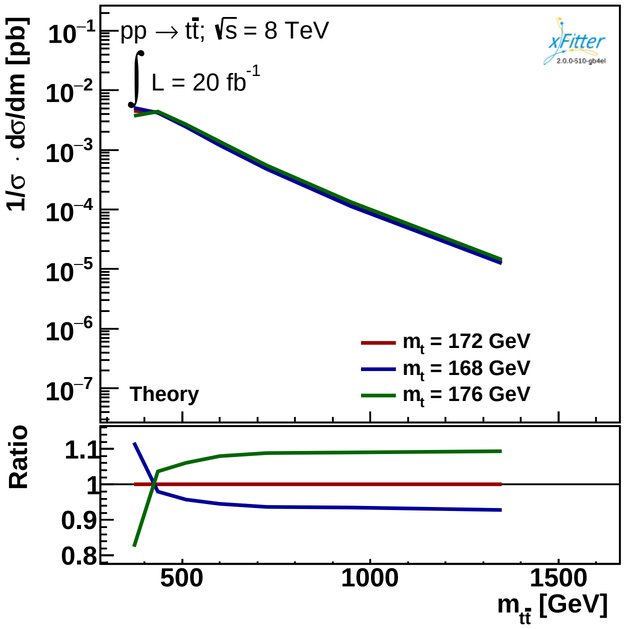

Figure 2: Normalised differential cross section against $m_{t\bar{t}}$ for 3 reference top quark mass points of 168, 172 and 176 GeV.

to NNLO using the ratio of NNLO to NLO predictions at the reference mass of m_t = 173.3 GeV.

This study uses the CT14NNLO PDF set and $\alpha_S = 0.118$. The PDF uncertainities are scaled from 90% to 68% confidence level and α_S is varied in the range $\pm$ 0.001. The missing predictions at higher order uncertainties are estimated through variations of the renormalisation and factorisation scales. Each scale is varied independently by factors of 2 and 0.5, and the corresponding cross section variations are added in quadrature. The QCD scale variations are evaluated at NLO. Since the predictions are corrected to NNLO, they yield a conservative estimate of the missing higher-order uncertainty.The PDF uncertainities and scale variations are included in the χ^2 as nuisance parameters.

Figure 3 shows NLO predictions at the reference mass of m_t = 173.3 GeV, including the PDF uncertainties and QCD scale variations and the total uncertainty-which is the quadratic sum of the two.

Figure 4 shows a comparison of `applGRID` predictions at m_t = 173.3 GeV with the `fastNLO` grids both at NLO and NNLO. This plot provides a benchmark of the two methods for creating the grids and exposes the key differences in the theory between NLO and NNLO. One can see that `fastNLO` at NLO is consistent with `applGRID`. On the contrary NNLO predictions are not consistent with NLO

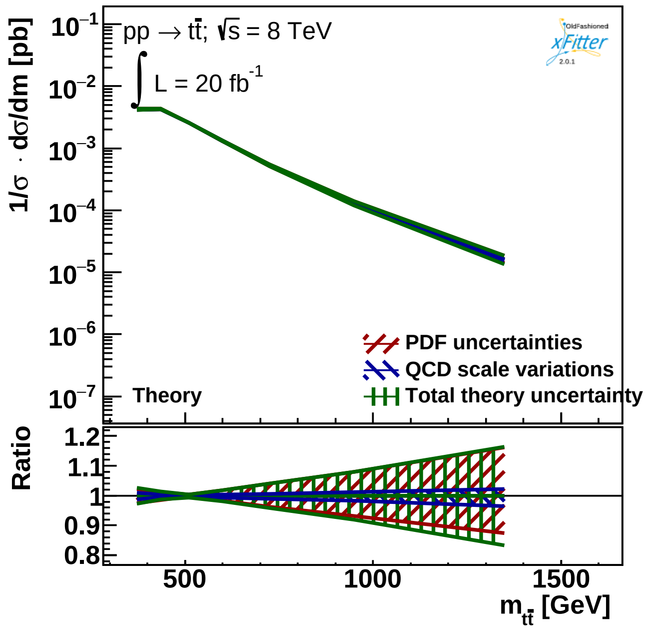

Figure 3: figure
Normalised differential cross section as a function of $m_{t\bar{t}}$ showing PDF uncertainties including α_S variations and QCD scale variations.

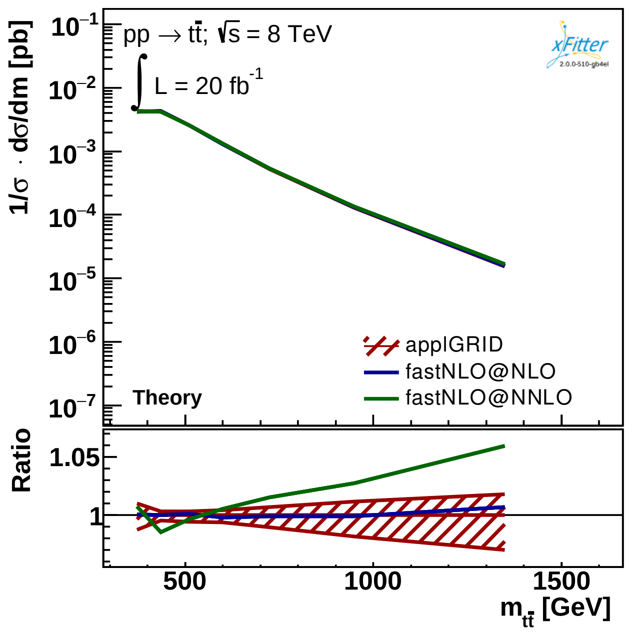

Figure 4: Comparison of `applGRID` and `fastNLO` grids

predictions, within the scale variation bands. This indicates that the α_s^4 corrections are significant and should be accounted for.

4 Correlation model for the experimental uncertainties

The measured differential cross section as a function of $m_{t\bar{t}}$ [8] used in this study is affected by various sources of uncertainties. They comprise the statistical uncertainty, and several sources of systematic uncertainty. The statistical uncertainty quoted for the normalised $m_{t\bar{t}}$ distribution in Ref.[8] does not include any bin-to-bin correlation. However a certain amount of (anti)correlation exists due to the normalisation procedure. In order to estimate the bin-to-bin statistical correlation of the normalised cross section, we have applied standard error propagation to the statistical uncertainty of the normalised differential cross section.

The bin width for which we are looking at the data is defined to be W_i, for the corresponding i^{th} bin. Measured differential cross section for the i^{th} bin is defined as $\partial\sigma^i_{t\bar{t}}$. Integrating over each bin we get the normalised cross section:

$$\sigma^i_{t\bar{t}} = W_i \cdot \partial\sigma^i_{t\bar{t}} \tag{1}$$

Taking the sum one obtains the total cross section for $t\bar{t}$ events:

$$\sum_i \sigma^i_{t\bar{t}} = \sum_i W_i \partial\sigma^i_{t\bar{t}} = \sigma^{total}_{t\bar{t}}. \tag{2}$$

The bin-integrated normalised cross sections for i^{th} bin ($\varsigma^i_{t\bar{t}}$) is defined by the ratio between the normalised cross section in bin i (Eqn 1) and the total cross section (Eqn 2):

$$\varsigma^i_{t\bar{t}} = \frac{\partial\sigma^i}{\sigma^{t\bar{t}}_{total}} = \frac{W_i \partial\sigma^i_{t\bar{t}}}{\sum_j \sigma^j_{t\bar{t}}} \tag{3}$$

$\varsigma^i_{t\bar{t}}$ for different bins i are statistically correlated unlike $\sigma^i_{t\bar{t}}$. The covariance matrix for the normalised uncertainties of $\varsigma^i_{t\bar{t}}$ is V where:

$$\mathbf{V} = \mathbf{G}\mathbf{S}\mathbf{G}^{\mathbf{T}} \tag{4}$$

S is the diagonal covariance matrix of the uncertainties s_i measured on $\sigma^i_{t\bar{t}}$. The diagonal elements are s_i^2 and off diagonal elements are trivially zero.
G is the matrix of partial derivatives $\mathbf{G}_{ij}$ where:

$$\mathbf{G}_{ij} = \frac{\delta_{ij}}{\sigma^{t\bar{t}}_{total}} - \frac{\sigma^{i}_{t\bar{t}}}{{\sigma^{t\bar{t}}_{total}}^{2}} \tag{5}$$

This method of calculating the statistical uncertainties can be used to calculate the systematic uncertainties as well. to the systematic uncertainties .

In calculating the normalised statistical covariance matrix for the normalised differential cross sections, one obtains the following correlation plot, ρ_{ij}. The largest correlation is -44%. It is negative as the number of events over all bins must be constant. Therefore the increase in events for bin i will lead to a decrease in events for bin j. It is the case for all correlation values ρ_{ij} where $i \neq j$, as seen in figure 5.

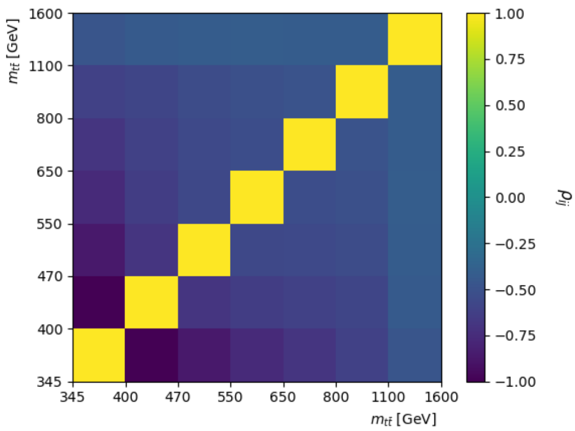

Figure 5: Statistical correlation matrix for normalised cross sections [8].

5 Closure test

The closure test is done to ensure when correlation values are included in the normalised differential cross sections, the uncertainties reduce, predominantly in the statistical uncertainty. To see this purely statistical effect, the χ^2 scan is performed on pseudo-data.

This is observed in figures 6 and 7 where the error range of the normalised differential cross sections reduces from ± 0.37 to $^{+0.30}_{-0.31}$, following the expected effect.

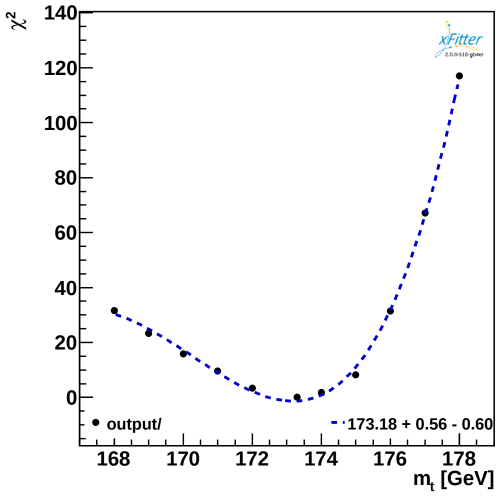

(a) χ^2 scan

	output
$m_t[GeV]$	173.18
Statistical	$+0.21-0.20$
Systematic	$+0.37-0.37$
PDFs	$+0.26-0.26$
QCD scales	$+0.15-0.15$
Total (decomposed)	$+0.52-0.52$
Total (from fit)	$+0.56-0.60$

(b) Output mass and uncertainties

Figure 6: $\chi^2(m_t = 173.3 \text{ GeV})$ for normalised differential cross sections

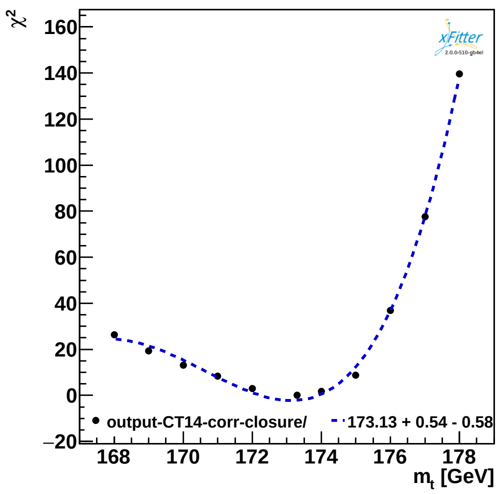

(a) χ^2 scan

	output
$m_t[GeV]$	173.13
Statistical	$+0.22-0.21$
Systematic	$+0.30-0.31$
PDFs	$+0.25-0.25$
QCD scales	$+0.14-0.14$
Total (decomposed)	$+0.47-0.47$
Total (from fit)	$+0.54-0.58$

(b) Output mass and uncertainties

Figure 7: $\chi^2(m_t = 173.3 \text{ GeV})$ for normalised differential cross sections

6 Blinding of data test

The blinding of data is completed by shifting the reference mass used to create the theory predication, grids. The method of blinding was by adding a shift to the reference value $m_{ref} + \Delta$ where Δ is a randomly generated shift. This value is in the range [-5, +5] GeV and created using the TRandom3 function on ROOT. This shift changes the reference mass in the input files used to create grids.

Figure 8 shows the χ^2 scan for the blinded pseudo-data grids for a prediction reference mass of 173.3 GeV. Looking at the central value found in this scan, it is 171.55 GeV which shows the central value has been shifted by -1.68 GeV, from 173.3 GeV. If the predicted mass is below the unblinded reference mass, Δ is postive, and vice versa. This is because all the grid files have been shifted in the direction of the shift and so the predicted value will shift in the opposite direction. When unblinding the data and revealing the shift value, one will find it to be +1.96469 GeV. With the inclusion of the uncertainties, the shift value is consistent with the values observed, successfully blinding the data.

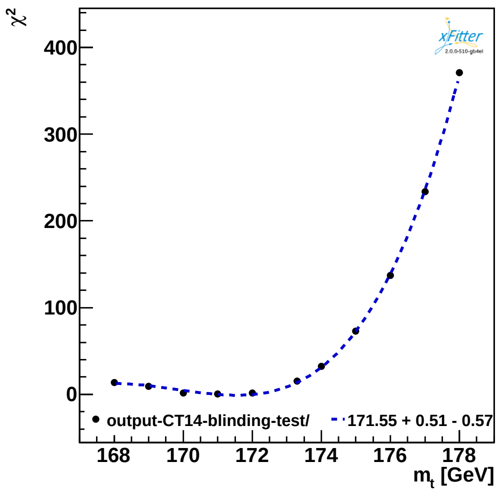

(a) χ^2 scan

	output
$m_t[GeV]$	171.55
Statistical	$+0.23-0.23$
Systematic	$+0.27-0.28$
PDFs	$+0.25-0.25$
QCD scales	$+0.15-0.15$
Total (decomposed)	$+0.46-0.47$
Total (from fit)	$+0.51-0.57$

(b) Output mass and uncertainties

Figure 8: $\chi^2(m_t = 173.3 + \Delta\text{GeV})$ for normalised differential cross sections

7 Results and Conclusion

Performing the analysis on the real blinded data both at NLO and NNLO allows one to observe the NNLO correction to NLO predicted top quark mass. The blinding used here is different to that in the blinding test performed on psuedo-data.

With the χ^2 scan at NLO, it was performed twice, once with the inclusion of both PDF + α_S and scale variations, and the second without scale variations, as seen in table 1. At NNLO the scale variations are never applied as they have not been scaled/normalised at NNLO. Analysis both with and without PDF uncertainties are performed, as seen in table 2.

χ^2 at minimum	2.20565
m_t [GeV]	177.79
Statistical	$+0.30-0.32$
Systematic	$+0.37-0.41$
PDFs	$+0.31-0.33$
QCD scales	$+0.19-0.20$
Total (decomposed)	$+0.60-0.65$
Total (from fit)	$+0.55-0.68$

(a) Inclusion of both PDF and QCD scale variations.

χ^2 at minimum	2.22205
m_t [GeV]	177.78
Statistical	$+0.30-0.31$
Systematic	$+0.37-0.41$
PDFs	$+0.31-0.33$
QCD scales	-
Total (decomposed)	$+0.57-0.61$
Total (from fit)	$+0.52-0.65$

(b) Inclusion of PDF uncertainties. No QCD scale variations included.

Table 1: χ^2 and m_t for NLO calculations with uncertainty decomposition

χ^2 at minimum	2.26185
m_t [GeV]	177.75
Statistical	$+0.31-0.32$
Systematic	$+0.39-0.42$
PDFs	$+0.32-0.34$
QCD scales	-
Total (decomposed)	$+0.59-0.63$
Total (from fit)	$+0.53-0.66$

(a) Inclusion of PDF uncertainties. No QCD scale variations included.

χ^2 at minimum	2.26209
m_t [GeV]	177.79
Statistical	$+0.29-0.30$
Systematic	$+0.36-0.39$
PDFs	-
QCD scales	-
Total (decomposed)	$+0.47-0.49$
Total (from fit)	$+0.43-0.52$

(b) No PDF uncertainties or QCD scale variations included.

Table 2: χ^2 and m_t for NNLO calculations with uncertainty decomposition

Table 1a shows the main result from this analysis and the central value of the top quark mass for which the χ^2 minimisation was found, m_t = 177.79 GeV. The NNLO correction to the uncertainty of the top mass is calculated by the mass shift in $\Delta m_t^{\mathrm{NNLO}}$ between table 1a and table 2a. The mass shift found was $\Delta m_t^{\mathrm{NNLO}}$= 0.031 GeV giving a final result of m_t = 177.79 $\pm$ 0.031 GeV. For the same two tables, the difference in the χ^2 = 0.041285, the NNLO correction to the χ^2 value.

The inclusion of the statistical correlation is a significant change when considering the statistical nature of the binning of events. This gives rise to a clearer understanding of the effects of the higher orders to the uncertainty of the mass of the top quark. Further considerations of also other physical effects such as the bound state effects, electroweak corrections will in turn lead to a more accurate understanding of the uncertainty decomposition and value of the top quark mass.

References

[1] G. Degrassi et al., Higgs mass and vacuum stability in the Standard Model at NNLO, JHEP 1208 (2012) 098, DOI: 10.1007/JHEP08(2012)098

[2] J. Haller et al., Update of the global electroweak ft and constraints on two-Higgs-doublet models, Eur. Phys. J. C 78 (2018) 8, 675, DOI: 10.1140/epjc/s10052-018-6131-3

[3] P Nason

[4]

[5] PDG 2019 http://pdg.lbl.gov/2019/tables/rpp2019-sum-quarks.pdf

[6] https://mcfm.fnal.gov/mcfm.pdf

[7] http://www.precision.hep.phy.cam.ac.uk/results/ttbar-fastnlo/

[8] http://cds.cern.ch/record/2102146/files/arXiv:1511.04716.pdf

[9] https://www.gnu.org/software/gsl/doc/html/montecarlo.html?highlight=vegas

[10] https://link.springer.com/article/10.1140